Time Lags and V–V' Steady States in the Infrared Laser Induced Decomposition of CHClF₂ and CDClF₂ under Collisional Conditions[1]

Ernest Grunwald,* Shu-Huei Liu, and Charles M. Lonzetta

Contribution from the Department of Chemistry, Brandeis University, Waltham, Massachusetts 02254. Received September 14, 1981

Abstract: V–T relaxation times of IR laser excited CHClF₂ are relatively long, being equivalent to ~400 gas kinetic collisions. IR laser induced decomposition of CHClF₂ yields CF₂ + HCl as primary products, as in thermal activation, for which E_{act} = 233 kJ/mol. Laser-induced decomposition at 15 and 50 torr is preceded by time lags that, when the absorbed energy is ≲70 kJ/mol, are several times longer than the 600 ns required for absorption of 95% of E_{absd}. As E_{absd} increases, the time lags decrease, and when $E_{absd} \gtrsim 140$ kJ/mol, they become <120 ns. Time lags for laser-induced decomposition of CDClF₂ are nearly the same as those for CHClF₂ decomposition at the same P and E_{absd}. These facts and others are shown to be consistent with the existence of V–V' steady-state equilibrium during V–T relaxation. A kinetic approach is developed in which the specific decomposition rate depends on the instantaneous *kinetic temperature*, which is expressed as a function of the vibrational-mode temperatures in the instantaneous V–V' steady state. The mode temperatures in turn depend on the dominant Δv selection rules for collisional V–V' exchange at the given vibrational energy. When $E_{absd} \lesssim 90$ kJ/mol, the observed time lags are reproduced by the S model, which, following Treanor et al.,[6] assumes that $\Delta v = \pm 1$. At higher E_{absd} ($\gtrsim 120$ kJ/mol), time lags are reproduced by the V model, which relaxes the Δv selection rules so that vibrational mode temperatures are all equal. Wider consequences for laser-induced nonthermal chemistry under collisional conditions are discussed in terms of this approach.

When infrared (IR) multiphoton excitation takes place under collisionless conditions, excited molecules can react only if they absorb enough photons to reach energy levels above the threshold for reaction. Under collisional conditions, however, IR excitation and collisional energy redistribution can cooperate, and in fact substantial reaction is known to occur even when the IR energy absorbed/mol (E_{absd}) is several times smaller than the activation energy (E_{act}) for thermal reaction.[2]

In this article we report a kinetic study of IR laser induced decomposition of CHClF₂ and CDClF₂ under collisional conditions, with special emphasis on reaction at relatively low excitation energies ($E_{absd}/E_{act} \geq 0.2$), and on the period including and right after the IR pulse in which nonthermal reaction can occur.

A brief description of terminology may be useful. Laser-induced reaction is said to be *thermal* when statistical equilibrium exists locally throughout the gas, so that each small macroscopic volume element can be assigned a characteristic temperature. (The local temperatures probably vary, both spatially and with time, because IR fluence, and hence E_{absd}, are nonuniform.) Laser-induced reaction is said to be *nonthermal* during the earlier period when the various modes of molecular motion (vibration V, rotation R, translation T) are relaxing toward a common temperature. In order to identify the nonthermal reaction period, one needs to know the time scale for relaxation to statistical equilibrium, especially the V–T relaxation time.

V–T relaxation rates of IR multiphoton excited CHClF₂ have been measured in this laboratory in CHClF₂–Br₂ mixtures, with the T–V rate of Br₂ as a temperature indicator.[3] An independent value in good agreement has been reported by Quack et al.[4] from studies of collisional deactivation by Ar in CHClF₂ molecules excited above the decomposition threshold. Details will be given in a later section.

It turns out that V–T relaxation times of CHClF₂ are relatively long, being equivalent to ~400 gas kinetic collisions. This is much longer than typical relaxation times for the exchange of vibrational energy *within* modes (V–V) and for dominant kinetic steps in

mechanisms of vibrational energy exchange *between* modes (V–V').[5,6] The relative time scales suggest that V–V and V–V' steady-state equilibrium exists during V–T relaxation. That is, the populations of the vibrational levels continually adjust so that V–V and V–V' exchange make net contributions of zero to the flow of molecular energy from vibration to translation.[7]

When the vibrational modes are harmonic, V–V exchange by hypothesis makes no contribution to the flow of molecular energy from V to T. It then follows that at steady-state equilibrium, the molecular distribution of any mode j can be characterized by a specific temperature T_j.[6] These mode temperatures vary with the progress of V–T relaxation. At any given time the different T_j's need not be equal but adjust so that V–V' exchange makes a net contribution of zero to the instantaneous flow of molecular energy from V to T.[6–8]

With the assumption that V–T relaxation, and hence nonthermal reaction, of CHClF₂ indeed proceeds with vibrational modes in V–V' steady-state equilibrium, two limiting cases will be of interest.

At low vibrational energies (and low vibrational-state densities) V–V' relaxation takes place largely in inelastic collisions. It has then been shown by Treanor et al.[6] for a specific mechanism and by Shamah and Flynn[8] for the more general case that in the V–V' steady state the mode temperatures T_j can vary widely and can be quite different from the T/R temperature T.

Let $v_1, v_2, ..., v_n$ and $v_1', v_2', ..., v_n'$ denote the vibrational quantum numbers of two molecules of the same substance before collision. The mechanism of Treanor et al.[6] assumes that collisional V–V' transfer proceeds with selection rule $\Delta v_j = -1$ and $\Delta v_k' = +1$, that is, with loss of 1 quantum of vibrational energy by any mode j in one of the molecules and gain of 1 quantum by a different mode k in the other molecule. In the V–V' steady state reached by this mechanism, temperatures (T_j, T_k, T) and normal-mode wavenumbers ($\bar{\nu}_j$, $\bar{\nu}_k$) for any pair of modes are related according to (1).[9,49]

$$\bar{\nu}_j(T_j^{-1} - T^{-1}) = \bar{\nu}_k(T_k^{-1} - T^{-1}) \qquad (1)$$

(1) This work was supported in part by a grant from the National Science Foundation and by equipment donated by the Edith C. Blum Foundation. S.H.L. gratefully acknowledges the award of a Gillette Fellowship.

(2) Dever, D. F.; Grunwald, E. *J. Am. Chem. Soc.* **1976**, *98*, 5055.

(3) Grunwald, E.; Lonzetta, C. M.; Popok, S. *J. Am. Chem. Soc.* **1979**, *101*, 5062.

(4) Quack, M.; Humbert, P.; van den Bergh, H. *J. Chem. Phys.* **1980**, *73*, 247.

(5) Weitz, E.; Flynn, G. *Ann. Rev. Phys. Chem.* **1974**, *25*, 275.

(6) Treanor, C. E.; Rich, J. W.; Rehm, R. G. *J. Chem. Phys.* **1968**, *48*, 1798, 1806.
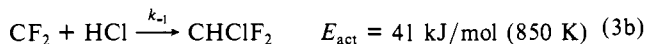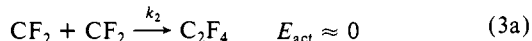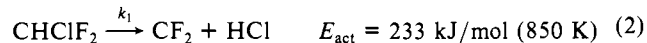
(7) Teare, J. D.; Taylor, R. L.; von Rosenberg, C. W. *Nature (London)* **1970**, *225*, 240.

(8) Shamah, I.; Flynn, G. *J. Chem. Phys.* **1978**, *69*, 2474.

There is good evidence that eq 1 is capable of describing at least a few real phenomena.[7,10]

At the opposite extreme, at high vibrational energies, one may assume that V–V' relaxation takes place with less stringent selection rules, mostly in intramolecular (i.e., unimolecular) processes[11] and in collisions that involve little or no exchange of T/R energy ($\Delta E_{T/R} \approx 0$). When V–V' steady state is reached under such conditions, the vibrational modes are all at the *same* temperature, which is different from the T/R temperature.[12]

Returning to the IR laser induced decomposition of CHClF$_2$, previous work under collisional conditions[13] has shown that the relevant reactions are (2)–(3), same as in thermal reaction, for

$$CHClF_2 \xrightarrow{k_1} CF_2 + HCl \qquad E_{act} = 233 \text{ kJ/mol (850 K)} \quad (2)$$

$$CF_2 + CF_2 \xrightarrow{k_2} C_2F_4 \qquad E_{act} \approx 0 \qquad (3a)$$

$$CF_2 + HCl \xrightarrow{k_{-1}} CHClF_2 \qquad E_{act} = 41 \text{ kJ/mol (850 K)} \quad (3b)$$

which rate constants and activation parameters are known.[14,15] Reaction 2 has also been used as a model process to pioneer the use of IR lasers in molecular dynamics, and energy partitioning in the collisionless decomposition of CHClF$_2$ at high fluence has been characterized.[16,17] Previous kinetic studies under collisional conditions mostly involve the decomposition of CHClF$_2$ at tracer concentrations in Ar at high fluence[4,18,19] and thus complement rather than overlap the present work. The only overlapping study, as far as we know, is that of Slater and Parks.[20] Their experiments do not include measurements of E_{absd} and thus cannot be compared directly with ours. Indirect comparisons reveal no marked inconsistencies.

Experimental Section

Materials. CHClF$_2$ gas (Freon 22) was obtained from Matheson Gas Products. The substance was distilled into a cold trap and outgassed three times prior to use. Purity was well over 99% by GLC analysis.

CDClF$_2$ was synthesized by photochemical reaction of chlorine gas with CD$_2$F$_2$ (Merck Canada) and isolated by preparative GLC in chemical purity of better than 99.9% and isotopic purity (with respect to CHClF$_2$) of ~99.9%. A full procedure has been reported.[21]

Normal Mode Wavenumbers.[22,23] CHClF$_2$: 3023, 1311, 1178, 809, 595, 422, 1347, 1116, 365. CDClF$_2$: 2265, 1015, 1163, 755, 593, 420, 972, 1106, 400. Wavenumbers listed for IR-active modes above 600 cm^{-1} are based on our own measurements.

Decadic molar extinction coefficients for analysis of gaseous substrates at room temperature were measured with a Perkin-Elmer Model 567 IR spectrophotometer. Results are listed in the format ϵ (M^{-1} cm^{-1}), wavenumber. CHClF$_2$: 121, 785; 173, 810; 363, 1095; 692, 1105; 225, 1120. CDClF$_2$: 86, 728; 110, 748; 50, 987; 47, 993; 61, 1010; 344, 1088; 398, 1099; 273, 1142; 268, 1155; 14, 2260. C$_2$F$_4$: 543, 1320; 603, 1330. CF$_2$: $\epsilon = 1000$ M^{-1} cm^{-1} at 249 nm; see Appendix.

Kinetic Measurements. CF$_2$ formation during and after an IR laser pulse was followed by kinetic absorption spectroscopy at 249 nm, essentially by methods described previously.[24] Two independent sets of data

Figure 1. Transmittance at 249 nm, observed with crossed IR and UV beams. The abscissa is time in μs. Thirteen torr of CHClF$_2$ in a 2.6-cm cell was irradiated at 1088 cm^{-1} with a short pulse; >95% of the fluence was delivered in 1.3 μs. The diameter of the IR beam was 1.73 cm and of the UV beam was $^1/_8$ in.; the cell diameter was 2.00 cm. E_{absd} was in the range 100–130 kJ/mol. Transmittance at 249 nm measures time evolution of CF$_2$ formed and reacting according to (2) and (3), with superposed gas dynamic effects.

were obtained, with significantly different instrumentation. The first set, by C.M.L., was obtained in 1977–1978. UV absorption was monitored by using an EMI 9798 QB photomultiplier and a Tektronix 7633 storage oscilloscope system with up to 60-MHz overall bandwidth. Data were processed photographically. IR intensity profiles of the laser pulses were measured with a Tachisto PDI photon-drag detector.

The second set, by S.H.L., was obtained in 1980–1981. In the interim, the CO$_2$ laser had been provided with a new grating and front optic, increasing coherence time of the radiation and giving sharper mode beats. UV absorption was monitored by using the faster but less sensitive EMI 9781 B photomultiplier. Data were acquired by a Biomation Model 8100 waveform recorder with an overall system bandwidth of about 15 MHz and were processed digitally. IR intensity profiles were measured with a Rofin 7401 photon drag detector.

Synchronization within 20 ns of UV and IR signals was achieved by using a photon drag detector to provide an appropriate trigger voltage during the quickly rising edge of the IR pulse. E_{absd} was measured by disk calorimetry, as described previously.[13]

The experiments by S.H.L. used a laser gas mixture that was lean in N$_2$ so that the IR intensity profiles were sharp, with relatively short tails. The experiments by C.M.L. used a laser gas mixture that contained about 30% more N$_2$ than that used by S.H.L., and a greater fraction of the IR pulse energy was present in the tail. Details are presented in Table I and in the caption of Figure 5.

Time Lags. The time when the photon drag detector first detects IR pulse intensity is taken as zero time. On this time scale, the "time lag for CF$_2$ formation" is taken as the time when the presence of CF$_2$ first becomes detectable by UV absorption spectroscopy. All measurements of time are corrected for instrumental delays.

Kinetic Deuterium Isotope Effects. Approximate activation parameters for use in kinetic model calculations were obtained as follows.

In the first experiment, a mixture of 26.65 torr of CDClF$_2$ and 16.95 torr of CHClF$_2$ was irradiated with an IR pulse at 1019 cm^{-1}, where CDClF$_2$ absorbs ($E_{absd} = 77.1$ kJ/mol of CDClF$_2$). A total of 1.75 torr of CDClF$_2$ and 1.52 torr CHClF$_2$ disappeared and an equivalent amount of C$_2$F$_4$ appeared.

In the second experiment, 33.91 torr of CDClF$_2$ and 9.49 torr of CHClF$_2$ was irradiated ($E_{absd} = 82.6$ kJ/mol of CDClF$_2$). A total of 3.56 torr of CDClF$_2$ and 1.22 torr of CHClF$_2$ was converted to C$_2$F$_4$.

Anticipating results to be presented, one may assume that the reaction is essentially thermal. On that basis, $k_H/k_D = 1.366$ at an averge $T = 898.6$ K in the first experiment and 1.233 at an average $T = 1048.7$ K in the second experiment. The average T is calculated from E_{absd} less a correction for reaction endothermicity[35] ($\Delta E° = 201$ kJ/mol for reaction 2) at the time when half of the stated amounts of the reactants have disappeared.

(9) Shamah, I.; Flynn, G. *J. Am. Chem. Soc.* **1977**, *99*, 3191. Mukamel, S.; Ross, J. *J. Chem. Phys.* **1977**, *66*, 35.

(10) (a) McNair, R. E.; Fulghum, S. F.; Flynn, G. W.; Feld, M. S. *Chem. Phys. Lett.* **1977**, *48*, 241. (b) Shamah, I.; Flynn, G. *J. Chem. Phys.* **1979**, *70*, 4928.

(11) McDonald, J. D. *Ann. Rev. Phys. Chem.* **1979**, *30*, 29.

(12) This is clear, for example, from ref 8, eq 20 (by letting $\Delta E = 0$) and can readily be derived on a more general basis.

(13) Grunwald, E.; Olszyna, K. J.; Dever, D. F.; Knishkowy, B. *J. Am. Chem. Soc.* **1977**, *99*, 6515.

(14) Edwards, J. W.; Small, P. A. *Nature (London)* **1964**, *202*, 1329.

(15) Barnes, R. G.; Cox, R. A.; Simmons, R. F. *J. Chem. Soc. B* **1971**, 1176.

(16) Sudbø, A. S.; Schulz, P. A.; Shen, Y. R.; Lee, Y. T. *J. Chem. Phys.* **1978**, *69*, 2312.

(17) Stephenson, J. C.; King, D. S. *J. Chem. Phys.* **1978**, *69*, 1485.

(18) Duperrex, R.; van den Berg, H. *J. Chem. Phys.* **1979**, *71*, 3613.

(19) Stephenson, J. C.; King, D. S.; Goodman, M. F.; Stone, J. *J. Chem. Phys.* **1979**, *70*, 4496.

(20) Slater, R. C.; Parks, J. H. *Chem. Phys. Lett.* **1979**, *60*, 275.

(21) Popok, S.; Lonzetta, C. M.; Grunwald, E. *J. Org. Chem.* **1979**, *44*, 2377.

(22) Plyler, E. K.; Benedict, W. S. *J. Res. Natl. Bur. Standards (U.S.)* **1951**, *47*, 202–220. Plyler, E. K.; Acquista, N. *Ibid.* **1952**, *48*, 92–97.

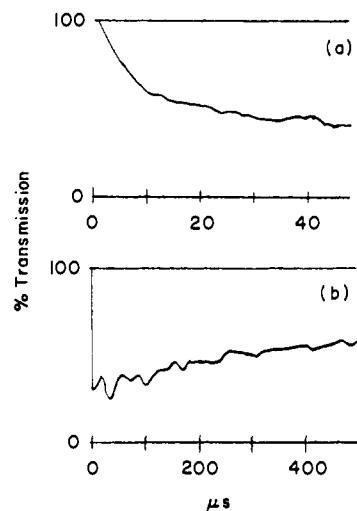(23) Milligan, D. E.; Jacox, M. E.; McAuley, J. H. *J. Mol. Spectrosc.* **1973**, *45*, 377–403.

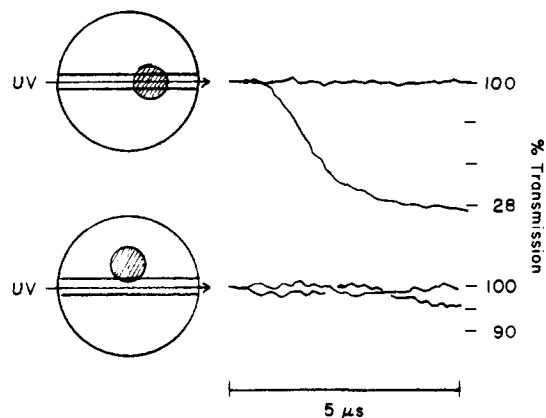(24) Garcia, D.; Grunwald, E. *J. Am. Chem. Soc.* **1980**, *102*, 6407.

Figure 2. Local CF_2 concentration as a function of time after IR-pulse excitation of 50 torr of $CHClF_2$ at 1088 cm^{-1} in a 0.4-cm cell; E_{absd} = 130 kJ/mol. The cell diameter (big circle) is 2.00 cm. The small shaded circle indicates the relative size and position of the IR beam. (Top) The UV monitoring beam intersects the region of IR irradiation. (Bottom) The UV beam is tangential to the region of IR irradiation. In the bottom trace, note the expanded transmittance scale and the several crossings of "control" and "IR" traces due to signal noise.

Letting $k_H/k_D = (A_H/A_D) \exp[-(E_{act}^H - E_{act}^D)/RT]$, we calculate from the above that $A_H/A_D = 0.646$ and $E_{act}^H - E_{act}^D = -5.60$ kJ/mol.

Control Experiments. The recent meticulous study by Duperrex and van den Bergh[18] reports a number of control experiments, many of which were also done independently in this laboratory. We found, in particular, that UV absorption at 249 nm is due to CF_2 and only CF_2, that local energy and temperature gradients in the IR-excited gas (due to nonuniform IR fluence) cause no detectable light scattering, and that possible surface effects involving the KCl cell windows are negligible. The second was shown by irradiating 14 torr of pure SiF_4 at 1025 cm^{-1}, where SiF_4 absorbs strongly,[25] and finding no change in the UV transmittance at 249 nm, where SiF_4 does not absorb significantly.

Response times of the measuring instruments, including electron transit times of the photomultipliers, were determined and corrected for. The region of linear response of the photomultipliers and related electrical circuitry was determined, and "overloading" was avoided.

The accuracy of intensity profiles measured with the photon-drag detector was checked by Dr. M. T. Duignan in this laboratory. Duignan built a plasma shutter that permits truncation of the IR pulses after a programmed delay. He found that $\int_0^t I(t')\, dt'$ as measured by the photon-drag detector was equal to the truncated pulse fluence $F(t)$ as measured by disk calorimetry.[48]

Gas Dynamic Effects. It is well-known that acoustic waves are generated when a gas is excited inhomogeneously by an IR laser pulse.[26,27] In the present case, fluctuations in CF_2 concentration will be seen as fluctuations in UV transmittance. Representative results obtained in two different experiments on different time scales are shown in Figure 1. Because the UV beam is perpendicular to the IR beam, the effect of acoustic waves traveling along the IR beam direction will clearly be important. However, waves traveling normal to the IR beam will also cause fluctuations, although they are probably smaller.

Of special interest in the present work is the mechanical behavior of the irradiated gas during and right after irradiation. Figure 2 shows that *during the first ~5 μs beginning with the IR pulse, the gas is mechanically quiescent*: The upper trace shows that IR irradiation under the given conditions produces a marked change in transmittance. The lower trace shows that this change does not expand appreciably into a volume element immediately adjacent. This evidence can be reinforced by similar results for other systems.[3,24] It appears that IR-irradiated gases remain mechanically quiescent during an initial period of 5–10 μs provided that (a) care is taken to use beams with approximately uniform fluence and (b) ~70% or more of the gas volume is irradiated.

Results

The remarkable feature of the IR laser induced decomposition of $CHClF_2$ under collisional conditions is that, at relatively low
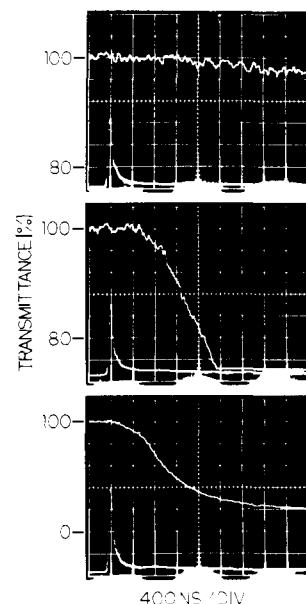
(25) Olszyna, K. J.; Grunwald, E.; Keehn, P. M.; Anderson, S. P. *Tetrahedron Lett.* **1977,** *19,* 1609.

(26) Bates, R. D.; Flynn, G. W.; Knudtson, J. T. *J. Chem. Phys.* **1970,** *53,* 3621.

(27) Burak, I.; Houston, P.; Sutton, D. G.; Steinfeld, J. I. *J. Chem. Phys.* **1970,** *53,* 3632.

Figure 3. UV transmittance vs. time at 249 nm, with IR-pulse profile shown underneath: (top) E_{absd} = 59 kJ/mol, lag 1400 ns; (middle) E_{absd} = 105 kJ/mol, lag 600 ns; (bottom) E_{absd} = 156 kJ/mol, lag 120 ns. A pressure of 15 torr of $CHClF_2$ was irradiated at 1088 cm^{-1}. The scale of the abscissa is 400 ns/division. For precise synchronization, the pulse profiles should be moved 30 ns to the left. The UV path length is 1.74 cm.

Table I. Fractions of Incident Fluence (f) and Absorbed Fluence (f_{absd}) as Functions of Time[a,b]

t, ns	$f(t)$	$f_{absd}(t)$	t, ns	$f(t)$	$f_{absd}(t)$
0	0.000	0.000	150	0.799	0.806
30	0.029	0.022	200	0.869	0.862
50	0.115	0.128	250	0.893	0.883
60	0.180	0.220	340	0.916	0.906
70[c]	0.269	0.328	530	0.951	0.945
80	0.380	0.444	730	0.980	0.974
90	0.485	0.548	990	0.997	0.998
100	0.574	0.630	1130	1.000	1.000
120	0.707	0.735			

[a] 25.1 torr of $CHClF_2$ was irradiated at 1088 cm^{-1}; E_{absd} = 12.1 kJ/mol; $\bar{F}$ = 0.076 J cm^{-2}; IR pulses are similar to those in Figure 3. [b] $f(t) = \int_0^t I_0(t')\, dt'/\int_0^\infty I_0(t')\, dt'$; $f_{absd}(t) = \int_0^t [I_0(t') - I_f(t')]\, dt'/\int_0^\infty [I_0(t') - I_f(t')]\, dt'$; $I_0(t'), I_f(t')$ = incident (transmitted) intensity of the absorbing gas at time t'. [c] Peak intensity.

values of E_{absd}, there are substantial time lags before CF_2 appears. (For the definition of "time lag", see the Experimental Section.) Representative results by S.H.L. are shown in Figure 3. In the experiment at the top, in which E_{absd} = 59 kJ/mol, the time lag is as long as 1400 ns even though more than 95% of the full E_{absd} is absorbed in 600 ns. As E_{absd} increases, the time lag decreases progressively, and in the experiment shown at the bottom in Figure 3 it is only 120 ns.

Table I shows the fractions of incident fluence (f) and of absorbed fluence (f_{absd}) as functions of time, calculated from photon-drag measurements of pulse intensity vs. time, in air and after passage through and ~50% absorption by $CHClF_2$. These data, obtained by S.H.L., are typical of results obtained in many experiments, at $CHClF_2$ pressures of 10–80 torr, and for E_{absd} up to >60 kJ/mol. f_{absd} exceeds 95% at 600 ns and 98% at 800 ns. (In C.M.L.'s experiments, f_{absd} exceeds 95% at 1100 ns and 98% at 1300 ns.) Differences between $f(t)$ and $f_{absd}(t)$ are fairly small in all experiments and may not be physcially real, because of ~10 ns jitter in the time-base trigger signal.

Figures 4 and 5 summarize results obtained independently by C.M.L. and S.H.L., with different instrumentation. Most of the experimental points are averages representing several experiments. The smooth curves labeled T, S, and V are model curves and will be described later.

Time Lags and V–V' Steady States in CHClF₂ and CDClF₂

J. Am. Chem. Soc., Vol. 104, No. 11, 1982 3017

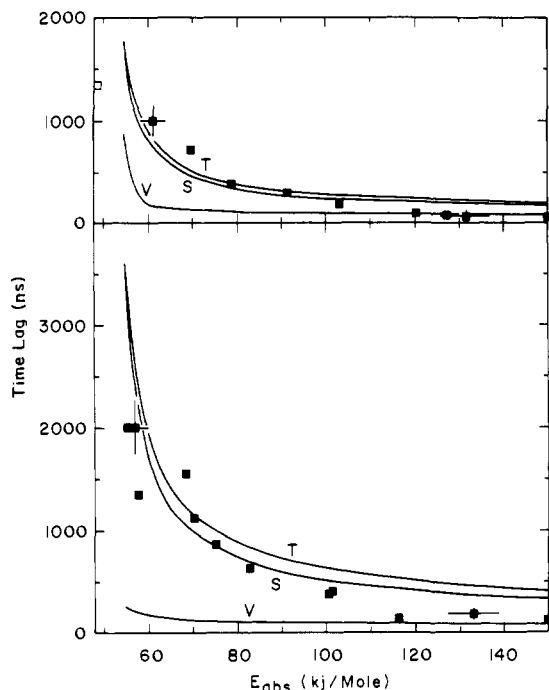**Figure 4.** Time lag vs. E_{absd} after IR irradiation at 1088 cm⁻¹: (top) 50 torr of CHClF₂; (bottom) 15 torr of CHClF₂. IR pulse shape is shown in Table I. Solid squares indicate measurements by S.H.L. Smooth curves indicate time lag predicted by T, S, and V models.

Figure 5. Time lag vs. E_{absd} for CHClF₂ (■) and CDClF₂ (□) after IR irradiation at 1088 cm⁻¹. Results are due to C.M.L.: (top) CHClF₂, 50 torr; CDClF₂, 44 torr; (bottom) CHClF₂, 15 torr; CDClF₂, 10–19 torr. Smooth curves indicate time lags for CHClF₂ predicted by T, S, and V models. IR pulse shape: t (ns), f; 70, 0.032; 130, 0.205; 220, 0.52; 500, 0.78; 1100, 0.95; 1300, 0.98; 1700, 1.00.

In spite of modest quantitative differences (time lags in C.M.L.'s series tend to be longer, at least in part because of the greater IR pulsewidths) the two series are essentially in agreement. In both series, time lags at 15 torr are substantially longer than at 50 torr (at the same E_{absd}), suggesting that the time lags can be traced back to collisional phenomena. At 15 torr, when $E_{absd} <$ 100 kJ/mol, both data sets lie close to the T- and S-model curves. At higher E_{absd} they approach the V model curve. At 50 torr, discrimination between T-, S-, and V-model curves is possible in S.H.L.'s experiments (Figure 4). When $E_{absd} <$ 90 kJ/mol, the data lie close to the T- and S-model curves; when $E_{absd} >$ 120 kJ/mol, they lie close to the V-model curve. In C.M.L.'s experiments at 50 torr, the data lie close to the model curves. But the model curves lie too close together, because of the greater IR pulsewidth, to provide further insights.

Also included in Figure 5 are time lags for CDClF₂ at pressures near 15 and 50 torr. The data show quite clearly, we think, that time lags for CDClF₂ are about the same as those for CHClF₂ at the same P and E_{absd}.

V–T Relaxation. In view of the evidence presented in the introduction,[6–10] it is reasonable to surmise that the time lags are due to the existence of V–V' steady states. This theory requires that the number of collisions involved in V–T relaxation be large compared to the typically small number required in rate-determining steps for collisional V–V' relaxation.

Accordingly, the kinetics of V–T relaxation of IR laser excited CHClF₂ was investigated.[3] Measurements were made with the same instrumentation as in the C.M.L. set of experiments. The method, its assumptions, and full results have been reported[3,28] and need not be repeated here. Some topics are worth mentioning, however.

(1) Because the substrate gas remains essentially at constant volume during the period of IR absorption, V–T relaxation, and initial reaction (Figure 2; also ref 3), the rate laws are conveniently written in terms of molar concentrations.

(2) The rate law for V–T energy relaxation of CHClF₂ was written in the form of (4),[3] where E_V = vibrational energy (above

$$\frac{dE_{V-T}}{dt} = \frac{E_V - E_V^{eq}(T)}{\sigma} \qquad (4)$$

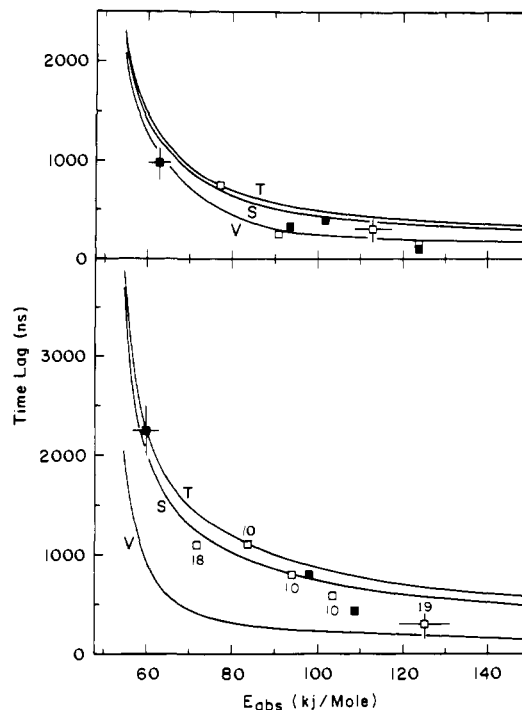the zero-point energy)/mol of CHClF₂ at time t, T = T/R tem-

perature, σ = V–T relaxation time at time t, and $E_V^{eq}(T)$ = vibrational energy/mol of CHClF₂ when statistical equilibrium exists at temperature T. Equation 4 is written so that $E_V(t)$ relaxes toward the instantaneous value of $E_V^{eq}(T)$.

(3) In principle, $\sigma(t)$ in (4) depends on concentration C, on the amount and distribution of E_V, and on T. However, within the achievable accuracy and 25% precision, σ^{-1} was given simply by (5), where C = molar concentration of CHClF₂ or, in case of

$$\sigma^{-1} = (1.0 \pm 0.2) \times 10^9 C \text{ s}^{-1} \qquad (5)$$

mixtures, effective molar concentration.[3,28] It should be stressed, however, that the method of measurement is indirect and cannot detect fine points of rate law.

In theory, at constant T, σ in (4) is constant for diatomic gases whose V–T relaxation follows the Landau–Teller transition probabilities[29,30] and for polyatomic gases whose V–T relaxation mechanism has a rate-determining step that follows the Landau–Teller transition probabilities. An example of the latter is the mechanism of Lambert and Salter,[31] in which the overall rate of V–T relaxation is defined by the V–T relaxation of the lowest frequency mode.

For diatomic gases, σ in (4) varies substantially with T according to empirical relationships whose form is predicted by Landau–Teller theory.[32] For the data of ref 3 for CHClF₂, however, the simple eq 5 gave a better fit than did relationships of the form used for diatomics.[32]

(4) In the experiments reported in ref 3, a representative average temperature of ≈700 K was used. Using kinetic theory to estimate the collision rate per CHClF₂ molecule at 700 K, it was found that the V–T relaxation time of CHClF₂ according to (5) is

(28) Correction: In Table I of ref 3, in experiment 3, $\sigma^{-1}C_{A,eff}^{-1}$ should be 0.94 × 10⁹ s⁻¹ M⁻¹. The mean and standard deviation for all CHClF₂ experiments should be (1.0 ± 0.2) × 10⁹ s⁻¹ M⁻¹.

(29) Landau, L.; Teller, E. *Phys. Z. Sowjet.* **1936**, *10*, 34. Ter Haar, D., Ed. "Collected Papers by L. D. Landau"; Gordon and Breach: New York, 1965.

(30) See, for example: Johnston, H.; Birks, J. *Acc. Chem. Res.* **1972**, *5*, 327.

(31) Lambert, J. D.; Salter, R. *Proc. Roy. Soc. A* **1959**, *253*, 277.

(32) Millikan, R. C.; White, D. R. *J. Chem. Phys.* **1963**, *39*, 3209.

equivalent to the time for ~ 400 gas-kinetic collisions.

Quack and co-workers[4] estimated recently, from decomposition rates of $CHClF_2$ in the presence of Ar, that for $CHClF_2$ molecules excited somewhat above the dissociation threshold (for which $E_V \approx 60$ kcal/mol) the mean amount of V energy transferred to T per collision with Ar molecules is 0.1 kcal/mol. This implies a V–T relaxation time equivalent to ~ 600 collisions.

The V–T relaxation time of $CHClF_2$ has also been measured at 298 K by ultrasonic dispersion[33] and is equivalent to ~ 1100 collisions.

Simple Models for Time Lags. Time delays or *incubation periods* preceding product formation are well known for IR laser induced reactions under collisionless conditions.[4,34] Such delays result from the time required to excite enough molecules sufficiently above the reaction threshold for the rate of reaction to become detectable. At the high fluences typical of *collisionless* reaction conditions, rates of IR absorption tend to exceed 1 photon/(molecule ns), and incubation periods are usually <50 ns.

The time lags observed in the present experiments in the lower energy range (>600 ns when $E_{absd} \lesssim 80$ kJ/mol and $E_{absd}/E_{act} \lesssim 0.35$) are clearly different from collisionless incubation periods. When $E_{absd}/E_{act} < 0.35$, it seems safe to predict that collisionless reactions would not be detectable. That is, the incubation period would be infinite.

In view of the relatively long V–T relaxation times of $CHClF_2$, it is reasonable to consider models involving V–V′ vibrational steady states. Time lags then result if the vibrational energy distributions in the steady states are unfavorable for reaction.

In constructing models to account for collisionless incubation periods it is desirable to use a detailed microscopic approach based on molecular dynamics. In constructing models to account for reaction rates in V–V′ steady states, however, the work of Shamah and Flynn[8] indicates that a macroscopic approach based on chemical kinetics will be adequate. We shall use such an approach.

The basic idea of our macroscopic approach is to retain the Arrhenius rate equation for nonthermal systems, but to replace T by a parameter T_k, called the *kinetic temperature*. In (6), k

$$k = A \exp(-E_{act}/RT_k) \qquad (6)$$

is the specific reaction rate and A and E_{act} are the Arrhenius parameters for *thermal* reaction. In nonthermal systems, T_k and k are functions of time. As statistical equilibrium is reached, T_k approaches T and k approaches the thermal rate constant.

The formulation of k according to (6) is convenient for those reactions, such as unimolecular decomposition, whose activation energy consists virtually entirely of vibrational energy. In that case T_k can be related to the temperatures of the vibrational modes in the V–V′ steady state, as well as to parameters of the activated complex. The relationship is especially simple when E_V is high enough so that, at steady states, all vibrational modes are at the same temperature T_V, which in the nonthermal system is different from the T/R temperature T. In that case $T_k = T_V$. A more general relationship will be obtained in the next section.

In this section we shall consider two simple models: the V-model assumes that all vibrational modes are at the same temperature T_V, so that $T_k = T_V$; the T model assumes that the vibrational steady state is such that $T_k = T$. Further simplification results because we are interested only in the initial reaction period so that (1) the degree of reaction $(1 - f_{CHClF_2}) \ll 1$ (f_{CHClF_2} = fraction of unreacted $CHClF_2$ at time t), (2) reaction 3 may be neglected, and (3) the endothermicity of reaction 2 is negligible compared to the absorbed IR energy $U_{absd}(t)$. The latter is conveniently written in the form of (7), where E_{absd} = energy absorbed/mol

$$U_{absd}(t) = E_{absd} f_{absd}(t) \qquad (7)$$

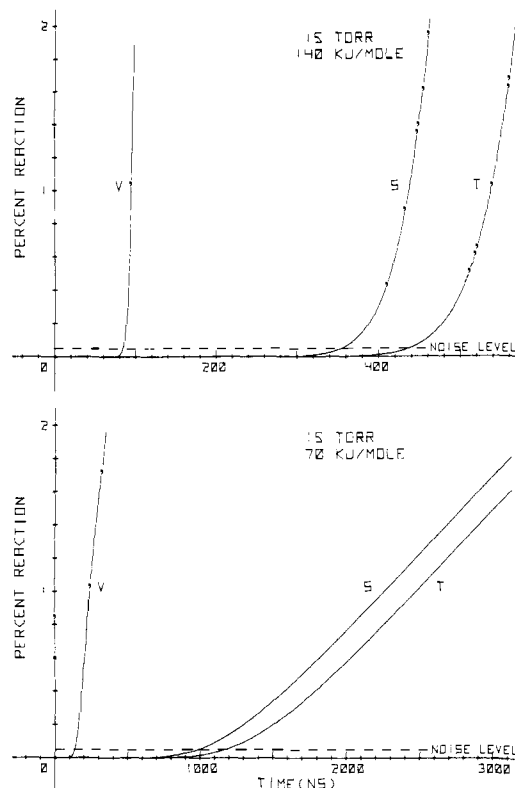from the *full* IR pulse and f_{absd} = fraction of E_{absd} absorbed at time t (Table I, note *a*).

Figure 6. Percent reaction vs. time calculated for 15 torr of $CHClF_2$ by using the IR pulse listed in Table I: (top) $E_{absd} = 140$ kJ/mol; (bottom) $E_{absd} = 70$ kJ/mol. Zero time corresponds to beginning of pulse. See text for description of V, S, and T models.

On this basis, and expressing the V–T/R rate according to (4), eq 8–10 express the rates of change of E_V, $E_{T/R}$, T, and f_{CHClF_2}.

$$\frac{dE_V}{dt} = E_{absd} \frac{df_{absd}}{dt} - \frac{E_V - E_V^{eq}(T)}{\sigma} \qquad (8)$$

$$\frac{dE_{T/R}}{dt} = C_{T/R}\frac{dT}{dt} = \frac{E_V - E_V^{eq}(T)}{\sigma} \qquad C_{T/R} = 3R \qquad (9)$$

$$-\frac{df_{CHClF_2}}{dt} = k(t) = A \exp(-E_{act}/RT_k) \qquad (10)$$

In solving these equations, we use (11) for the V model and (12)

$$\frac{dT_k}{dt} = \frac{dT_V}{dt} = (C_{E_V})^{-1}\frac{dE_V}{dt} \qquad \text{V model} \qquad (11)$$

$$\frac{dT_k}{dt} = \frac{dT}{dt} \qquad \text{T model} \qquad (12)$$

for the T model. C_{E_V} in (11) is the vibrational heat capacity at temperature T_V. σ is given by (5), $A = 6.92 \times 10^{13}$ s^{-1}, and $E_{act}/R = 28\,080$.[14] In the calculations of $E_V^{eq}(T)$ and C_{E_V}, we use normal-mode wavenumbers given in the Experimental Section and standard equations of statistical thermodynamics.[35]

Equations 8–12 were solved by numerical integration to give percent reaction $[100(1 - f_{CHClF_2})]$ as functions of time for representative values of E_{absd}. Plots based on the V model and the T model for $E_{absd} = 70$ and 140 kJ/mol are shown in Figure 6. The time lags are taken as the points at which *percent reaction* crosses the "noise level", which is based on the experimental detection limit for change in UV transmission due to CF_2 formation.

Smooth curves showing predicted time lag vs. E_{absd} are included in Figures 4 and 5. For the curves in Figure 4, data for f_{absd} vs.

(33) Rossing, T. D.; Legvold, S. *J. Chem. Phys.* **1955**, *23*, 1118.
(34) Yahav, G.; Haas, Y.; Carmeli, B.; Nitzan, A. *J. Chem. Phys.* **1980**, *72*, 3410.

(35) (a) "JANAF Thermochemical Tables", 2nd ed.; NSRDS-NBS 37, June 1971 (U.S. Gov. Printing Office No. C 13.48:37); pp 9–10. (b) Wavenumbers listed for $CHClF_2$ differ significantly from those of ref 22, as follows: 836 instead of 1178; 400 instead of 365.

time are those in Table I and are representative of IR pulses employed by S.H.L. For the curves in Figure 5, the data for f_{absd} vs. time represented the somewhat wider pulses employed by C.M.L.

It is clear, especially from Figure 4, that the observed time lags approach those predicted by the V model in the upper range of E_{absd}, above $\sim$120 kJ/mol. In theory one would expect mode temperatures of vibrational steady states to be described accurately by the V model when E_V becomes sufficiently high, say when the density of vibrational states becomes $\gtrsim$1/wavenumber. For CHClF$_2$, such a density is reached when $E_V \sim$40 kJ/mol. In experiments in which $E_{absd} \gtrsim$ 120 kJ/mol, E_V becomes >40 kJ/mol after <70 ns during the IR pulse.

In the lower range of E_{absd} the V model fails badly, but the T model fits rather well. One should *not* infer from this, however, that the reaction rate depends directly on the translational energy but rather *that vibrational-mode temperatures during V–T relaxation vary in such a way that T_k remains close to T.*

Model of Specific-Mode Temperatures (S Model). A credible model for the lower range of E_{absd} can be constructed on the basis of eq 1. In this model, the vibrational-mode temperatures are unequal, and one therefore needs an expression that relates kinetic temperature to temperatures of the individual modes. Because collisional conditions exist, we shall assume that kinetic conditions approach those in the high-pressure limit of the unimolecular reaction mechanism.[36] Under such conditions, Slater theory[36,37] provides a convenient framework for the derivation.

Kinetic Temperature. Let ϵ_V denote the vibrational energy of a given molecule and $\epsilon_1, ..., \epsilon_j, ..., \epsilon_n$ denote the component modewise energies. Let $\epsilon_{V,0}$ denote the critical vibrational energy for reaction. According to Slater theory,[37] there are two modewise energy requirements for reaction: condition 13 specifies the

$$\epsilon_V = \sum_{j=1}^{n}\epsilon_j \geq \epsilon_{V,0} \qquad (13)$$

$$\sum_{j=1}^{n}(\alpha_j^2\epsilon_j/\epsilon_{V,0})^{1/2} \geq 1 \qquad (14a)$$

$$\sum_{j=1}^{n}\alpha_j^2 = 1 \qquad (14b)$$

necessary minimum for the total energy; condition 14 specifies how ϵ_V must be distributed among the vibrational modes in order that excitation be along the reaction coordinate q. In (14), α_j is the direction cosine of q with respect to the normal coordinate Q_j, and positive square roots are taken.

Since the temperatures of the vibrational modes are unequal, by hypothesis, the modewise energy distribution requirement (14) is of special interest. In particular, one might ask whether (13) and (14) imply minimum energy requirements not only for the molecule as a whole but also for individual modes.

When $\epsilon_V = \epsilon_{V,0}$, the answer is "yes". One finds, by minimizing $\sum\epsilon_j$ by the method of Lagrange multipliers[38] subject to the constraints (13) and (14), that any mode j has a fixed and definite energy requirement $\epsilon_{j,0}$, related to α_j and $\epsilon_{V,0}$ according to (15). In view of (14b), $\sum\epsilon_{j,0} = \epsilon_{V,0}$.

$$\epsilon_{j,0} = \alpha_j^2\epsilon_{V,0} \qquad (15)$$

When $\epsilon_V > \epsilon_{V,0}$, the modewise energy requirements for reaction are no longer fixed and definite, and (15) is no longer a unique solution. However, modewise distributions in which ϵ_j for any mode j is substantially smaller than $\epsilon_{j,0}$ that also satisfy (14) occur with low statistical probability. This is because such reactions proceed, in effect, through distorted transition states with enhanced critical energies, leaving less energy disposable for statistical distribution among the other modes. In the following, reaction

events in which $\epsilon_j < \epsilon_{j,0}$ will be neglected.

The probability that a harmonic oscillator in an ensemble at temperature T_j will have an energy $\epsilon_j \geq \epsilon_{j,0}$ is $\exp(-\epsilon_{j,0}/kT_j)$. The probability that a molecule with n independent harmonic modes in an ensemble with distinct mode temperatures $T_1, ..., T_j, ..., T_n$ will satisfy simultaneously the conditions $\epsilon_1 \geq \epsilon_{1,0}, ..., \epsilon_j \geq \epsilon_{j,0}, ..., \epsilon_n \geq \epsilon_{n,0}$ similarly is (16).

$$\exp(-\epsilon_{1,0}/kT_1) \times ... \times \exp(-\epsilon_{j,0}/kT_j) \times ... \times \exp(-\epsilon_{n,0}/kT_n) \qquad (16)$$

The species of molecules described by (16), in the terminology of Robinson and Holbrook,[36] is the activated complex, and such molecules react with a probability per second that is independent of the underlying vibrational-energy distribution. To the approximation of the Arrhenius equation, the reaction probability per second is also independent of T. The specific reaction rate is therefore given by (17), where A is the Arrhenius A factor. On introduction of the reasonable approximation that $E_{act} = N_0\epsilon_{V,0}$ and comparison of the result with (6), the kinetic temperature is found to be (18).

$$k = A \exp[-\sum_{j=1}^{n}\epsilon_{j,0}/kT_j] \qquad (17)$$

$$T_k^{-1} = \sum_{j=1}^{n}(T_j^{-1}\epsilon_{j,0}/\epsilon_{V,0}) \qquad (18)$$

Application to CHClF$_2$. In the probable transition state for HCl elimination from CHClF$_2$, the C–H and C–Cl bonds are partially broken and the H–Cl bond is partially formed. Although in principle all nine vibrational modes are coupled to the reaction coordinate, the nominal C–H stretch (3023 cm^{-1}) and C–Cl stretch (809 cm^{-1}) should be the most important. Of the two, the C–H stretch should be more important than the C–Cl stretch, because the C–H stretching force constant is 50% greater and because the amount of C–H stretch required in the transition state is almost certainly larger.

In consideration of the above, we shall represent kinetic temperature for reaction 2 simply and arbitrarily by (19).

$$T_k^{-1} = 0.8T_{3023}^{-1} + 0.2T_{809}^{-1} \qquad (19)$$

Specific Mode Temperatures (S Model). This model uses eq 8 and 9 to obtain E_V and T as functions of time. Given E_V and T at a given t, eq 1 is solved by successive approximations to obtain the temperatures T_j of the individual modes. Equation 19 then evaluates T_k, and calculation of $\int k\, dt$ by numerical integration according to (10) gives the desired relationship of f_{CHClF_2} vs. t. Sample plots resulting from such calculations are included in Figure 6, and smooth curves showing time lag vs. E_{absd} are included in Figure 4 and 5. The calculations are lengthy and require 10–50 min of Hewlett-Packard Model 9825 A calculator time for a plot of f_{CHClF_2} vs. t to obtain a time lag.

It is clear from Figures 4–6 that time lags predicted by the S model are only slightly shorter than those of the T model. The physical basis for this similarity is as follows. First, in the V–V' stationary states according to (1), the temperatures of high-wavenumber modes are not much different from T. Second, the temperature of the C–H stretching mode at 3023 cm^{-1}, according to (19), makes the dominant contribution to the kinetic temperature. 3023 cm^{-1} is the highest normal-mode wavenumber of CHClF$_2$.

Time Lags for CDClF$_2$. In view of the importance of C–H stretching in the transition state for CHClF$_2$ decomposition, it is reasonable to characterize the observed time lags, when $E_{absd} \lesssim$ 90 kJ/mol, as periods during which the mean energy of the C–H stretching mode is well below the statistical average. A consistent explanation, as we have seen, assumes the existence of V–V' steady states, with collisional selection rules (at low E_{absd}) so that high-wavenumber modes, such as the C–H stretch, remain at temperatures near T. In this model V–V' exchange between the C–H stretch and other modes is kinetically "fast".

An alternative model that can lead to time lags assumes that V–V' exchange between the C–H mode and other modes is spe-

(36) (a) Robinson, P. J.; Holbrook, K. J. "Unimolecular Reactions"; Wiley: New York, 1972; pp 275–281. (b) *Ibid.*; p 40. (c) *Ibid.*; Chapter 2.

(37) Slater, N. B. "Theory of Unimolecular Reactions"; Cornell University Press: Ithaca, NY, 1959; Chapter 5.

(38) Margenau, H.; Murphy, G. M. "Mathematics of Physics and Chemistry"; Van Nostrand: New York, 1943; p 205.

3020 *J. Am. Chem. Soc., Vol. 104, No. 11, 1982*

Grunwald, Liu, and Lonzetta

Table II. Model Time Lags (ns) for $CHClF_2$ and $CDClF_2$[a]

E_{absd}, kJ/mol	$CHClF_2$			$CDClF_2$		
	V	S	T	V	S	T
		15 torr			18 torr	
70	445	*1330*	1510	700	*1384*	1580
80	340	*1040*	1215	416	*1025*	1200
125	*190*	592	705	206	537	660
		50 torr			44 torr	
70	740	*910*	960	913	*1067*	1145
80	434	*655*	712	525	*738*	812
125	*198*	352	394	208	370	428

[a] Same IR pulse shape as in Figure 5. Time lags based on preferred model are shown in italics. The pressures are those of the actual experiments.

cifically "slow". Such a model was of interest to us especially during the early stages of this work, when the possibility of mode-selective chemistry as a result of modal differences in V–V′ exchange rates above the reaction threshold was being widely discussed.[11,39-43] We were hoping that an examination of deuterium isotope effects might be instructive.

Figure 5 shows time lags observed in the IR laser induced decomposition of $CDClF_2$. Under comparable conditions, the time lags are quite similar to those observed for $CHClF_2$. Although the facts may not be completely decisive, the following model calculations do show good consistency with the V–V′ steady-state hypothesis. These calculations were made on the same basis as those for $CHClF_2$ but by using $CDClF_2$ normal-mode wavenumbers and rate constants derived from those for $CHClF_2$ and from k_H/k_D as listed in the Experimental Section. The C–D stretch and C–Cl stretch in $CDClF_2$ are at 2265 and 755 cm^{-1}, respectively. V–T relaxation was treated according to (4) and (5).

Time lags predicted in this way for $CDClF_2$ are compared with those for $CHClF_2$ in Table II. Although the V-, S-, and T-models all predict a difference under comparable conditions, time lags predicted by the S-model at low E_{absd} and by the V-model at high E_{absd} are so similar for the two substrates that, were they true to reality, our experiments could not detect the difference. We conclude that the experiments with $CDClF_2$ further strengthen the evidence in favor of the V–V′ steady-state hypothesis.

The experiments with $CDClF_2$ also indicate that reaction during the initial period is not thermal. If reaction were thermal, $CDClF_2$ would have reacted more slowly, and time lags would have been longer.

Reaction Kinetics after the Time Lag. When $[CHClF_2] = 0.027$ M (50 torr at 298 K), V–T relaxation is nearly complete after 2 μs, whereas the IR-excited gas remains mechanically quiescent for 5–10 μs. It is therefore possible to test whether reaction following V–T relaxation is thermal. To do so, one needs to plot $[CF_2]$ rather than optical density vs. time, and one needs to modify eq 8–10 to include (a) the effects of endothermicity of reaction 2 and (b) the stoichiometric and energetic effects of reactions 3.

The determination of ϵ for CF_2 at the monitoring wavelength of 249 nm under actual experimental conditions is described in the Appendix. For the sake of precision we shall use our own value, even though its accuracy is not claimed to be superior to that of prior determinations.[18,44-46]

In fitting the data for $[CF_2]$ vs. time, the quality of fit is limited by the accuracy of E_{absd}, which is measured with a standard error of 5%. We therefore devised a nonlinear least-squares treatment in which E_{absd} was adjusted near the experimental value until a least-squares fit of $[CF_2]$ vs. time during the mechanically quiescent period was obtained. Calculations involving six of

C.M.L.'s experiments at 50 torr, selected to cover the full range of E_{absd}, gave least-squares parameters for E_{absd} that differed from measured values by +1.5 ± 3.0%. A similar analysis for six $CDClF_2$ experiments at 44 torr gave E_{absd} parameters differing from measured values by −2.0 ± 3.0%. The standard errors of fit of $[CF_2]$ at the least-squares optimum averaged <3% for $CHClF_2$ and <4% for $CDClF_2$, expressed as percent of the amount of CF_2 reached at the end of the ~5-μs period of fit. It seemed justified to conclude that reaction after completion of V–T relaxation is thermal and proceeds with thermal rate constants.

Discussion

Our kinetic results for $CHClF_2$ and $CDClF_2$ support the theory that during V–T relaxation following IR absorption, the vibrational modes exist in V–V′ steady states. At low E_{absd} (≲90 kJ/mol), the steady-state-mode temperatures are characteristically different, in such a way that the specific decomposition rate is strikingly smaller than expected for the same amount of vibrational energy at statistical equilibrium. One observes time lags preceding reaction that, near the detection limit for reaction, are as long as 3–4 times the V–T relaxation time. Under these conditions the time lags are reproduced quite well by the S model, which assumes that C–H bond stretching accounts for most of the activation energy and that V–V′ steady states are reached through inelastic collisions by the mechanism of Treanor et al.[6] in which the colliding molecules gain or lose 1 vibrational quantum in one mode at a time.

At higher E_{absd} (≳120 kJ/mol), the temperatures of the vibrational modes tend to become equal, probably because additional mechanisms for V–V′ exchange become significant. Under these conditions the time lags are reproduced quite well by the V model, which assumes that all vibrational modes are at the same temperature. Prior to completion of V–T relaxation after IR absorption, this vibrational temperature (and hence the kinetic temperature) is higher than the T/R temperature and the specific decomposition rate is greater than it would be in a thermal system with the same amount of energy. This latter fact has been pointed out.[20,47]

It seems likely that the kinetic behavior found for $CHClF_2$ and $CDClF_2$, following IR absorption under collisional conditions, is of some generality. If so, one may ask whether new kinds of nonthermal chemistry can be designed.

The V model, which fits at high E_{absd}, predicts genuine differences from thermal chemistry during V–T relaxation only if translational and/or rotational energy make an important contribution to the activation energy. When this is not the case, however, there may still be useful effects due to the high vibrational and hence high kinetic temperatures.

In V–V′ steady states during V–T relaxation at lower E_{absd}, the vibrational-mode temperatures are specifically different, and genuine differences from thermal chemistry are readily envisaged. According to (18), T_k depends not only on $\{T_j\}$ but also, through $\{\epsilon_{j,0}/\epsilon_{v,0}\}$, on the transition-state structure. Different reaction paths, with different transition states, will have different $\{\epsilon_{j,0}/\epsilon_{v,0}\}$ and thus different kinetic temperatures. Given an appropriate distribution of mode temperatures, it is conceivable that reaction paths that are unimportant in thermal systems now may become important.

When V–V′ steady states develop according to eq 1, differences in mode temperatures can be quite large. Low-wavenumber modes will have high T_j's and high-wavenumber modes will have T_j's that are fairly close to T. Reactions in which low-wavenumber modes make important contributions to $\epsilon_{v,0}$ will be facilitated.

In unimolecular decomposition it is probable, however, that such cases are rare. Activation energies tend to be dominated by bond stretching rather than bond bending and thus tend to be facilitated by high temperatures in modes of high rather than of low wavenumber. If so, the time-lag behavior of $CHClF_2$ and $CDClF_2$

(39) Sloane, C. S.; Hase, W. L. *J. Chem. Phys.* **1977**, *66*, 1523.
(40) Oxtoby, D. W.; Rice, S. A. *J. Chem. Phys.* **1976**, *65*, 1676.
(41) Thiele, E.; Goodman, M. F.; Stone, J. *Opt. Eng.* **1980**, *19*, 10.
(42) Kaldor, A.; Hall, R. B.; Horsley, J. A.; Kramer, G. M.; Rabinowitz, P. *J. Am. Chem. Soc.* **1979**, *101*, 4465.
(43) Oref, I.; Rabinovitch, B. S. *Acc. Chem. Res.* **1979**, *12*, 166.
(44) Dalby, F. W. *J. Chem. Phys.* **1964**, *41*, 2297.
(45) Modica, A. P. *J. Phys. Chem.* **1968**, *72*, 4594.
(46) Tyerman, W. J. R. *Trans. Faraday Soc.* **1969**, *65*, 163.

(47) Grunwald, E.; Lonzetta, C. M.; Olszyna, K. *J. ACS Symp. Ser.* **1977**, *56*, 107.
(48) Duignan, M. T. Ph.D. Thesis, Brandeis University, Waltham, MA, 1982.

Table III. Evaluation of ϵ for CF$_2$ at 249 nm

$2[C_2F_4]_f$, mM	t_1, ms	$(OD)_{t_1}$	$10^{-4} \times$ slope,^{a} s^{-1}	$10^{-7} \times 2k_2$, s^{-1} M^{-1}	ϵ(eq 21), M^{-1} cm^{-1}
0.0169	1.6	0.0221	1.5^c	3.1	874
0.164	0.6	0.126	1.1^d	3.3	921
0.0197	1.6	0.0236	1.8^c	4.0	938
0.117^b	0.1	0.280	1.1^d	3.9	1021
0.272^b	0.2	0.334	1.0^d	3.4	1043
0.200^b	0.2	0.311	1.0^d	3.7	1156

^{a} Slope of $(OD)^{-1}$ vs. t when $t \geqslant t_1$. Slope = $2k_2/\epsilon l$. ^{b} Experiments with CDClF$_2$. Other experiments involve CHClF$_2$. ^{c} $l = 2.36$ cm. ^{d} $l = 3.26$ cm.

at low E_{absd} should be rather typical.

Appendix

Molar Extinction Coefficient of CF$_2$ at 249 nm. While there was only marginal need to know the ϵ of CF$_2$ for the interpretation of time lags, a semiquantitative value was needed to show that after V–T relaxation, reaction indeed becomes thermal reaction. It is known that ϵ changes slowly with T.[45] However, for the present purposes it seemed adequate to treat ϵ as constant. On that basis ϵ could be derived from (a) a plot of optical density (OD) at 249 nm vs. time and (b) the amount of C$_2$F$_4$ produced. At 249 nm, CF$_2$ is the only component of the reacting system whose optical absorption is significant. The rate law for C$_2$F$_4$ formation is d[C$_2$F$_4$]/dt = k_2[CF$_2$]^2, where k_2 is nearly independent of T.[14,15,44,46]

After a sufficiently long time t_1 has elapsed, the gas temperature becomes low enough (<900 K) so that reversible decomposition of CHClF$_2$ (eq 2 and 3b) is practically quenched, according to available kinetic data.[14,15] Thus, when $t > t_1$, the sole reaction is (3a). The condition $t > t_1$ can be recognized experimentally because the decrease of OD with t then follows second-order kinetics; the slope of the straight-line plot of $(OD)^{-1}$ vs. t equals $2k_2/\epsilon l$ where l is the optical path length of the UV beam.

Let [CF$_2$]$_1$ denote [CF$_2$] at $t = t_1$ and let [C$_2$F$_4$]$_f$ denote the final C$_2$F$_4$ concentration. The initial [C$_2$F$_4$] = 0, and when $t > t_1$ further reversible formation of CF$_2$ from CHClF$_2$ is negligible. We may therefore write (20). Change of variable to OD and

$$2[C_2F_4]_f = [CF_2]_1 + \int_0^{t_1} 2k_2[CF_2]^2 \, dt \qquad (20)$$

rearrangement yields (21). $(OD)_{t_1}$ and $2k_2/\epsilon l$ are known from

$$\epsilon = \left[(OD)_{t_1} + (2k_2/\epsilon l) \int_0^{t_1} (OD)^2 \, dt \right] \Big/ (2[C_2F_4]_f l) \qquad (21)$$

the plot of $(OD)^{-1}$ vs. t when $t \geq t_1$. $(OD)^2 \, dt$ is evaluated by numerical integration of optical density data for $0 \leq t \leq t_1$. Given l and $[C_2F_4]_f$, ϵ can therefore be determined.

Results for several experiments are listed in Table III. Precision of 10% is attained. The accuracy is lower, however, because the period of integration $0 \leq t \leq t_1$ includes the period of mixing of irradiated with nonirradiated gas when the UV path length l is not well defined. Final averages are ϵ (base 10) 1000 ± 200 cm^{-1} M^{-1} at 249 nm (monochromator FWHM $\sim$ 2 nm) and $2k_2 = (3.6 \pm 0.7) \times 10^7$ s^{-1} M^{-1} at $\sim$800 K.

Registry No. CHClF$_2$, 75-45-6; CDClF$_2$, 1495-14-3; C$_2$F$_4$, 116-14-3; CF$_2$, 2154-59-8.

---

(49) Professor Colin Steel has obtained a particularly simple derivation of eq 1. Consider collisional V–V' exchange according to (22). This is a

$$A^* + B \underset{k_r(T)}{\overset{k_f(T)}{\rightleftharpoons}} A + B^* \qquad (22)$$
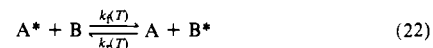
state-to-state process only for vibrational states. Translational and rotational energies follow a statistical distribution dependent on the T/R temperature T. Hence k_f and k_r are rate constants dependent on the T/R temperature T of the ensemble, and $k_f(T)/k_r(T) = \exp(-[E_B - E_A]/kT)$. Let $T_{V,A}$ and $T_{V,B}$ denote "temperatures" defined by the relative populations A*/A and B*/B, respectively. At thermal equilibrium (eq) $T_{V,A} = T_{V,B} = T$. Thus $([A^*]/[A])_{eq} = \exp(-E_A/kT)$ and $([B^*]/[B])_{eq} = \exp(-E_B/kT)$. The V–V' steady state (ss) is defined so that $k_f(T)([A^*][B])_{ss} = k_r(T)([A][B^*])_{ss}$. Furthermore, $([A^*]/[A])_{ss} = \exp(-E_A/kT_{V,A})$ and $([B^*]/[B])_{ss} = \exp(-E_B/kT_{V,B})$. Thus in the steady state, $\exp(-E_B/kT_{V,B})/\exp(-E_A/kT_{V,A}) = \exp(-[E_B - E_A]/kT)$, which reduces to (1).

A Valence Bond Effective Hamiltonian for Neutral States of π Systems. 1. Method

J.-P. Malrieu* and D. Maynau

Contribution from the Laboratoire de Physique Quantique, E.R.A. 821, Université Paul Sabatier, 31062 Toulouse Cedex, France. Received March 2, 1981

Abstract: An N-electron topologically determined Hamiltonian is proposed. It results from the application of the quasi-degenerate many-body formalism to the VB-CI matrix where the neutral configurations are considered as the nearly degenerate perturbed subspace. At the second order, ionic configurations perturbatively introduce an effective (negative) exchange integral between bonded atoms, resulting in a single parameter Heisenberg Hamiltonian. A general recurrence formula is given for the higher orders corrections, which only introduce a second parameter. Due to the cancellation of unlinked contributions, the effective operators are only concerned with connected fragments of the molecular graph; they essentially result in a small effective exchange integral between nonadjacent atoms and important cyclic contributions for even rings (allowing two or three simultaneous spin exchanges along the cycle).

This paper presents an effort to find an effective N-electron Hamiltonian which might give some information about *several states* of the N-electron systems. Such information is especially desired when the lowest states become nearly degenerate and the efforts to improve a prefered single determinant (as done in the Hartree–Fock scheme) seem rather arbitrary. π-Electron systems have been chosen as a test case for a strategy consisting of building an effective VB-type Hamiltonian restricted to a class of VB configurations, and taking benefit of the powerful tool known as

the "quasi-degenerate many-body perturbation theory".[1] The QDMBPT approach may be used first as a numerical tool for searching several quasi-degenerate roots in ab initio CI problems.[2] It may also be used to treat in a rational way the effect of a

---

(1) B. H. Brandow, *Rev. Mod. Phys.*, **39**, 771 (1967) See also J. des Cloizeaux, *Nucl. Phys.* **20**, 321 (1960); I. Shavitt and L. T. Redmon, *J. Chem. Phys.*, **73**, 5711 (1980).
(2) D. Hegarty and M. A. Robb, *Mcl. Phys.*, **37**, 1455 (1979).